Title: Hydrological modelling of climate change impacts on river flows in Siberia's Lena River Basin and implications for the Atlantic Meridional Overturning Circulation

Short title: Climate change impacts on discharge of Siberia's Lena River

C.E. Hudson[1] and J.R. Thompson[1]

[1]UCL Department of Geography, University College London, Gower Street, London, WC1E 6BT (charlotte.hudson.15@ucl.ac.uk)

A hydrological model of Siberia's Lena River Basin is calibrated and validated against observed river discharge at five stations. Implications of the Representative Concentration Pathway 4.5 scenario for river discharge are assessed using projections from 41 Coupled Model Intercomparison Project Phase 5 General Circulation Models grouped into 12 genealogical-based groups as well as a group ensemble mean. Annual precipitation increases in all scenarios (1.7–47.4%). Increases in annual PET are of a similar range (6.0–45.5%). PET peaks in June compared to July for the baseline. All temperature changes exceed 1.5°C (range: 2.2–6.2°C). The largest absolute increases are in winter (maximum +7°C). Changes in mean annual discharge range from -8.5–+69.9%. Ten GCM groups and the group ensemble mean project increases. Earlier snowmelt is dominant so the annual flood peaks in May compared to June for the baseline. Increased discharge of the Lena and other Eurasian rivers to the Arctic Ocean has the potential to impact Atlantic Meridional Overturning Circulation (AMOC). Enhanced fluxes for four groups are capable of weakening the AMOC. Changes for other groups may contribute to weakening when combined with other sources of freshwater and warmer temperatures.

Keywords: AMOC, climate change, CMIP5, Lena, RCP4.5

INTRODUCTION

Climate change will intensify the global hydrological cycle. Modified precipitation patterns coupled with changes in temperature and evapotranspiration will have important implications for river discharge (Vihma *et al.* 2016). The most severe hydrometeorological impacts of rising temperatures are being observed in, and are projected for, the Arctic, with mean annual air temperatures between 2001 and

2012 being 1.5°C warmer than during 1971–2000 (Overland *et al.* 2013). Precipitation is increasing and is projected to be >50% higher by 2100. Winter warming is projected to be four times greater than summer warming, modifying snowmelt, evapotranspiration and ultimately river discharge (Ye *et al.* 2004).

Reported increases in Arctic river flows have raised concerns about the integrity of the Atlantic Meridional Overturning Circulation (AMOC; Shu *et al.* 2017). AMOC comprises northward flows of warm saline water, formation of North Atlantic Deep Water (NADW) through sinking due to buoyancy loss, and southward return flows of cold deep-water (Buckley and Marshall 2016). Palaeoclimate proxy records (e.g. Broecker *et al.* 1985; Clark *et al.* 2002) suggest that the AMOC has collapsed in the past pointing to the potential for it having stable 'on' and 'off' states. Simulations from simple numerical models (e.g. Manabe and Stouffer 1988; Hawkins *et al.* 2011) support the presence of this bi-stable behaviour suggesting that it may collapse in the future. Enhanced freshwater input into the Arctic Ocean could reduce surface water density and potentially inhibit the formation of deep water, causing a positive feedback whereby reduced NADW formation decreases northward transport of saltwater further reducing water density and therefore convection. However, studies using coupled General Circulation Models (GCMs) to assess AMOC alterations have not identified this instability, and the most recent consensus of the IPCC is that AMOC slowdown is more likely than complete collapse during the 21st Century (Kirtman *et al.* 2013).

The implications of a weakening or collapse of AMOC would be widespread due to global-scale teleconnections (Vellinga and Wood 2008). Climatic implications may include North Atlantic cooling, an equatorward shift of the Inter-Tropical Convergence Zone and weakened monsoons (Buckley and Marshall 2016). AMOC collapse may also increase water resources stress in Europe and southern Asia due to altered precipitation patterns (Gosling 2013). Additionally, reductions in the extent of boreal and temperate forests are projected, with implications for carbon storage in these latitudes (Köhler *et al.* 2005). Fisheries and crop yields could be negatively impacted due to changes in ocean circulation with the potential for major societal implications (Keller *et al.* 2000; Kuhlbrodt *et al.* 2009). Given the significance of changes in AMOC, this study investigates the potential impacts of climate change upon river flows within Siberia's Lena River Basin, a major contributor of freshwater to the Arctic. Results are

scaled up to assess the potential implications for the AMOC of changes in Eurasian runoff to the Arctic Ocean.

STUDY AREA: THE LENA RIVER BASIN

The Lena River (Figure 1), which enters the Arctic Ocean via the Laptev Sea, is located in northern Asia and originates in the Baikal mountains (maximum altitude: 1,640m). It is the eleventh longest river in the world (4,400 km) with the ninth largest basin (32,000 km^2) (Gelfan *et al.* 2017). As the second largest Eurasian river in terms of discharge, following the Yenisei and preceding the Ob, the Lena provides around 15% of total mean annual runoff to the Arctic Ocean (mean annual discharge: 524km^3; Shiklomanov *et al.* 2000; Ye *et al.* 2004) although it varies from year to year.

The Lena Basin lies in a zone of continental moderate and sub-arctic climate (Liu and Yang 2011). Precipitation is highest during April–October (total precipitation at Yakutsk = 152mm), peaking in July and subsequently decreasing during November–March (total precipitation at Yakutsk = 78mm). Mean annual precipitation (based on CRU TS4.01) varies from 402 mm over the Tabaga sub-catchment to 280 mm over Stolb. This downstream decline is repeated for temperature with mean annual temperature (CRU TS4.01) decreasing from -8°C over Tabaga to -17°C over Stolb. Temperature and evapotranspiration peak in July, after which snow accumulation commences, reaching a maximum extent in November, before snowmelt begins in March (Ye *et al.* 2003).

The lowest and highest river flows occur during winter and summer, respectively. Snowmelt during May causes rapid increases in discharge, which on average peaks in June (Gelfan *et al.* 2017). Permafrost underlays 93% of the basin and directs precipitation and snowmelt to rivers. It contributes to low sub-surface storage capacity, causing large differences between winter and summer flows (Ye *et al.* 2004). The Lena has three main tributaries, the Aldan, Upper Lena and Vilui (Figure 1). The Aldan experiences peak flows that are approximately 60 times the lowest flows in April. Relatively higher high- and low-flows are experienced in the Upper Lena so that the ratio of highest to lowest flows is 26 (Ye *et al.* 2003). The Vilui contributes a relatively small amount to annual runoff (9% of discharge). The reservoir on this tributary (completed in 1967) has a capacity equivalent to 7% of annual runoff. Whilst it increases

81 winter flows above natural levels (Ye *et al.* 2003), these account for just 10% of annual discharge, and
82 the higher summer flows are relatively unaffected (Holmes *et al.* 2012).

83 The basin is sparsely populated and vegetation is largely natural comprising forests (84%), shrublands
84 (9%), grasslands (3%), croplands (2%) and wetlands (1%) (Liu and Yang 2011). Forests dominate the
85 southwest and tundra dominates the north. Whilst the basin's water resources are utilised for domestic
86 purposes, hydropower and irrigation, total use comprises a very low percentage of mean annual runoff
87 (Berezovskaya *et al.* 2005). The impacts of climate change can therefore be more easily identified and
88 are likely to dominate future changes as opposed to anthropogenic activities.

89 Temperature and precipitation have increased across the basin, especially during the cold season
90 (November–April; Dzhamalov *et al.* 2012). Changes in river discharge include earlier seasonal peaks and
91 larger flows in spring, summer and winter in contrast to autumn declines. A significant upward trend
92 (up to 90%) at the basin outlet (Stolb) during low-flow periods has been recorded whilst slight increases
93 (5–10%) in high-flows have been observed (Ye *et al.* 2003). Recognition that climate change may have
94 already impacted Lena River discharges, combined with the important role these flows and those from
95 other Eurasian rivers play in the global climate system, provides the impetus for assessing potential
96 future changes within the current study.

97 **METHODS**

98 **Model development, calibration and validation**

99 This study employs a coupled hydrological/hydraulic model of the Lena River Basin developed using
100 the MIKE SHE / MIKE 11 modelling system. MIKE SHE is commonly described as a deterministic, fully
101 distributed and physically based hydrological modelling system although it includes a range of process
102 descriptions, some of which are more conceptual and semi-distributed in nature (Refsgaard *et al.* 2010).
103 MIKE SHE is dynamically coupled to MIKE 11, a 1D hydraulic model that represent channel flow (e.g.
104 Thompson *et al.* 2004). Model development for the Lena Basin followed approaches used in other large
105 river systems (e.g. Andersen *et al.* 2001; Thompson *et al.* 2013). Table 1 summarises the model set-up
106 and the data it employs. Basin extent was determined using the USGS GTOPO-30 DEM with the lowest
107 point defined as Stolb. A cell size of 10km × 10km (total cells: 24680) was employed with GTOPO-30

being used to define the elevation of each grid cell. The saturated zone was represented using linear reservoirs, a conceptual, semi-distributed approach particularly applicable to large river systems where the focus is river flow simulation (Andersen *et al.* 2001). The Lena was divided into five sub-catchments (defining the extent of a series of saturated zone linear reservoirs – see below; Figure 1) based on the GTOPO-30 DEM and the location of gauging stations used for model calibration and validation. Stations were selected based on length and completeness of discharge records within the Regional Arctic Hydrographic Network (R-ArcticNET) dataset. Each sub-catchment was further sub-divided according to elevation into zones of approximately equal size (14 in total) representing the highest, intermediate and lowest zones. These were specified as interflow reservoirs whilst two baseflow reservoirs representing faster and slower baseflow storage were specified beneath each sub-catchment. The two time constants (interflow and percolation) for each interflow reservoir and the baseflow time constant for each baseflow reservoir, which control exchanges between reservoirs and the MIKE 11 hydraulic model, were varied during calibration.

The unsaturated zone was simulated using the two-layer water balance method. Spatial distribution of soil types was based on the FAO Digital Soil Map of the World (v3.6, 2003) with groups aggregated into three textural classes; 'fine', 'medium/fine', and 'coarse'. Hydraulic parameters were taken from Atwell *et al*. (1999). Land cover was based on the USGS Global Land Cover Characterisation dataset (GLCC). The dominant classes, including deciduous needle-leaf forest, bare rock, and tundra, were retained. Remaining classes were aggregated into groups of similar characteristics including water, croplands and grasslands, broadleaf forest, needle-leaf evergreen shrubs and bogs. For each, Root Depth (RD) and Leaf Area Index (LAI) were obtained from Arnell (2005). Permafrost was not included in the model as this is not a feature of MIKE SHE. This is common to a number of other hydrological models that have been used to assess the impacts of climate on river flows including within high latitude basins such as the Lena (e.g. Gosling *et al.* 2017; Veldkamp *et al.* 2018).

To account for variations in climate, the areas defining the extent of the five saturated zone linear reservoirs were further divided into a total of 19 smaller areas herein referred to as meteorological sub-catchments. The discretisation of these areas was based on their ranges in latitude, longitude and

elevation as well as the major tributaries within each saturated zone linear reservoir sub-catchment (Figure 1). Time-series of mean monthly precipitation and monthly maximum and minimum temperatures were derived for each meteorological sub-catchment from the CRU TS4.01 dataset (Harris *et al.* 2014). Since R-ArcticNET data used in model calibration and validation comprised mean monthly discharge necessitating the aggregation of simulated mean daily discharge for comparison, precipitation was distributed evenly and temperatures assumed constant on a daily basis through each month. Whilst this is acknowledged to be a simple approach, it follows earlier work undertaken using MIKE SHE and other hydrological models in similarly large river basins that demonstrated insensitivity to alternative temporal disaggregation of meteorological data when simulation results are aggregated to mean monthly discharges (e.g. Kingston *et al.* 2011; Thompson *et al.* 2013). Following approaches in other mountainous settings, varying precipitation lapse rates were applied over these sub-catchments (Ji and Luo 2013) and were subject to calibration but kept within the bounds used elsewhere (Immerzeel *et al.* 2012; Thompson *et al.* 2014). CRU TS4.01 temperatures for each meteorological sub-catchment were used to calculate Hargreaves potential evapotranspiration (PET; Hargreaves and Samani 1985). MIKE SHE then calculates actual evapotranspiration (AET) using the evaporative demand (PET), crop coefficients and the available soil moisture. PET, as for precipitation, was evenly distributed through each month on a daily basis. This PET method is recommended as an alternative to Penman-Monteith in cases of limited data availability (Allen *et al.* 1998) and has been used in similar studies (e.g. Ho *et al.* 2016; Thompson *et al.* 2017a). Snowmelt was simulated using a degree-day method and meteorological sub-catchment averaged CRU TS4.01 temperature. As for precipitation, temperature lapse rates were specified within each meteorological sub-catchment.

A digitized channel network defined the MIKE 11 river branches comprising the main river channels. All branches were specified as coupled to MIKE SHE. Cross-sections were established using channel widths obtained from Google Earth and estimated maximum depths based on similar studies (Thompson *et al.* 2014). The Vilui reservoir was excluded from the section of the MIKE 11 model within this sub-catchment due to a lack of data and its small influence on the annual discharge (Holmes *et al.* 2012).

R-ArcticNET discharge data were separated into two periods, 1960–1979 and 1980–1999, for calibration and validation, respectively. In both cases the previous year was used as a spin-up period. Calibration was undertaken from upstream to downstream by adjusting the parameters defined above (principally the saturated zone linear reservoir time constants and lapse rates). As previously indicated, simulated river discharges, which were stored at the maximum model time step of 24 hours, were aggregated to mean monthly discharge for comparison with the R-ArcticNET data. Model performance was assessed visually and statistically using the Nash-Sutcliffe efficiency coefficient (NSE), bias (Dv) and the Pearson correlation coefficient, (r). Performance based on the values of these three statistics was further classified into one of five classes (ranging between "very poor" and "excellent") using the scheme of Ho *et al.* (2016) which was itself adapted from Henriksen *et al.* (2003).

Climate change scenarios

Precipitation and minimum and maximum temperatures were obtained for the 41 GCMs of Phase 5 of the Climate Model Intercomparison Project (CMIP5) and the Representative Concentration Pathway (RCP) 4.5 scenario as it represents the most likely increase in global temperatures (UNFCCC 2015). The use of an ensemble of climate models enables assessment of the magnitude of GCM-related uncertainty (Ho *et al.* 2016). Using the mean output from a range of GCMs to force a hydrological model is thought to provide a more reliable representation of future conditions than the output from a single GCM. However, this assumption only holds if the GCMs are independent of one another (Pirtle *et al.* 2010). This is not strictly the case for the CMIP5 ensemble since GCMs developed by different institutions share literature, parameter values and some model code and the ensemble includes multiple versions of some GCMs or numerous GCMs from a single institution. The potential for biases due to this lack of model independence were addressed by grouping the 41 GCMs according to their genealogy using 12 groups (Ho *et al.* 2016; Table 2).

Mean monthly maximum, mean and minimum temperatures and precipitation were obtained for each meteorological sub-catchment for the baseline (1961–1990) and scenario (2071–2100) periods for all 41 GCMs. This 30-year scenario period was selected to represent conditions towards the end of the 21st Century (e.g. Thompson *et al.* 2017b). The baseline is of identical length and incorporates most of the

period used in model calibration / validation but excludes the latter part of the 20th Century during which changes in meteorological networks may impact model performance (discussed below). Mean values were then obtained from the GCMs in each of the 12 groups. Monthly differences (°C for temperature, % for precipitation) between baseline and scenario meteorological conditions were calculated for each GCM group for each of the meteorological sub-catchments. These differences, referred to as delta factors, were subsequently used to perturb the original CRU TS4.01 precipitation and temperature data and then Hargreaves PET was re-calculated. The delta factor approach ensures that scenario time-series retain the baseline climate variability and are not affected by any biases inherent within an individual GCM (Anandhi *et al.,* 2011). An additional group ensemble mean scenario was established using the same approach and employing the mean monthly baseline and scenario temperatures and precipitation from the 12 groups.

RESULTS

Model calibration and validation

Figure 2 demonstrates the generally good model performance. Timings of low and high flows are well represented, with slightly earlier increases in simulated discharges at Kusur and Stolb. Annual peaks are well reproduced upstream. Although the model is less successful at simulating low flows at Vilui towards the end of the period (most likely due to the dam), the rising and recession limbs are well represented. This generally superior upstream performance is further demonstrated by the observed and simulated river regimes (mean monthly discharge) for each gauging station and the calibration, validation and baseline periods.

NSE for the calibration period is classified as 'excellent' at two stations and 'very good' at the remaining three (Table 3). Lower NSE values at Kusur and Stolb are related to poorer representation of peak discharges. It was not possible to increase peaks without impacting the annual rise and recession, and ultimately increasing the overall bias. Since a focus of this study is the volume of water flowing into the Arctic Ocean, calibration focused on achieving a good match between observed and simulated mean flows. The bias for one station (Tabaga) was classified as 'excellent', whilst for the remaining stations it

was 'very good'. The values of r were variable as calibration was a compromise between achieving higher r values and smaller biases.

NSE values for the validation period are 'excellent' or 'very good' at all stations but Vilui where winter flows are underestimated. A shift from overestimation, or small underestimation, during the calibration period, to underestimation during the validation period is evident. Dv values ranged from 'good' at Tabaga, Aldan and Stolb, to 'poor' at Kusur and Vilui. This poorer performance may be related to changes in meteorological networks and how well they represent the Lena's climate. These factors (discussed below) may have been particularly acute towards the end of the 20th Century. If so, they are less likely to impact the baseline period against which climate change results are compared. NSE for this period is classified as 'very good' for three stations, and 'good' for two (Table 3). Dv is classified as 'excellent' at four stations, and 'very good' at the remaining station. Figure 2 confirms the generally very good performance of the model for this period.

Projected climate

Mean annual precipitation, temperature and PET are projected to increase for all GCM groups across the Lena Basin (Figure 3). The magnitude of these changes varies between groups and sub-catchments. Seasonal patterns of change are also variable, most prominently at higher latitudes, where some groups (2, 6, 8, 9, 10 and 11) project a second precipitation peak in October in addition to the July baseline peak. In general, but with the exception of Group 5, larger increases in precipitation are projected downstream. The largest increase in annual precipitation across all groups and sub-catchments is 47.4% (Group 9, sub-catchment r) whilst the smallest is 1.7% (Group 4, sub-catchment d). Group 10 is associated with the largest inter-sub-catchment range (11.9–45.1%) and Group 7 the smallest (12.5–20.7%). Changes for the group ensemble mean range between 15.0% and 27.5% (mean: 19.7%).

All temperature increases exceed the 2015 Paris target of 1.5°C (UNFCCC 2015) varying between 2.2°C and 6.2°C (mean: 2.7°C). The greatest absolute increases are projected during winter (maximum 6.2°C, Group 9, sub-catchment r). The duration of the period when temperatures are above freezing extends by, on average, one month, most prominently at higher latitudes. Group 9 is associated with the largest increases (mean: 5.4°C), including earlier seasonal gains in temperature. Group 10 again has the largest

242 inter-sub-catchment range of change (2.0°C). In contrast, groups 4 and 5 project relatively small
243 increases (2.2°C–3.2°C and 2.2°C–3.5°C, respectively). Increases in temperature for the group ensemble
244 mean range between 3.2°C and 4.4°C (mean: 3.7°C).

245 Increases in mean annual PET are of a similar range, albeit slightly smaller, to those of precipitation
246 (6.0–45.5% across all GCM groups and sub-catchments). The smallest increases are predominantly
247 projected by Group 5 (6.0–15.2%, mean: 10.9%) whilst Group 1 generally produces the largest increases
248 (24.7–34.5%; mean: 27.8%). The range for the group ensemble mean is 15.5–24.2% (mean: 19.2%). All
249 groups and the group ensemble mean project basin-wide peaks in June, one month earlier than for the
250 baseline (although the largest absolute changes occur in May; Figure 3).

251 **Projected river discharge**

252 Changes in discharge are generally consistent with 10 of the 12 groups and the group ensemble mean
253 projecting increases at all gauging stations. These increases are, however, of variable magnitude (Figure
254 4). Across the basin changes range between -8.5% to +36.8%. Groups 1, 3 and 5 project the largest basin-
255 wide increases. Declines are limited to groups 4 and 12, which project declines at four (-8.5–-1.0%) and
256 five (-5.8–-1.7%) stations, respectively. These groups are associated with relatively large increases in
257 PET (8.0–19.0% and 18.1–26.2%, respectively) that exceed increases in precipitation (1.7–17.2% and
258 9.6–19.5%, respectively). The group ensemble mean projects increases in mean discharge of between
259 5.6% and 18.6% (mean: 10.1%) with the increase of 9.2% for Stolb, indicative of Arctic Ocean inflow,
260 contrasting with the range for the 12 groups of -5.3%–21.7%. All but two groups (again 4 and 12) are
261 associated with increases in these flows.

262 High (Q5) and low (Q95) flows also increase for most groups. Changes in Q5 across all groups and
263 gauging stations range between -2.8 and +69.9%. Increases are, in percentage terms, larger than those
264 for mean annual discharge. Declines are again limited to groups 4 (three stations) and 12 (one station).
265 However, they are small compared to most increases. The group ensemble mean projects increases in
266 Q5 at all stations (range: 10.2–30.2%). Q95 increases in most cases with relatively small (≤6.7%)
267 declines limited to just two stations for Group 4 and one for groups 2 and 12. The small (2.8%) decline
268 for Tabaga projected by Group 2 is the only reduction in any discharge measure beyond groups 4 and

12. These two groups project the smallest increases in Q95 (<8.2%) whilst groups 1, 3 and 5 project some of the largest (up to 41.7%, Group 3, Aldan). Increases in Q95 of between 15.7% and 28.0% are projected by the group ensemble mean.

Projected river regimes (Figure 5) show that in many cases the seasonal peak advances to May compared to June under baseline conditions. This is most pronounced for groups 9 and 10, both of which project large basin-wide increases in temperature, and Group 11 and the group ensemble mean at Vilui. Group 9 projects the most pronounced change at Stolb with mean May discharge being 82% larger than the baseline. For many groups the recession limb declines more rapidly so that discharges in September are lower than during baseline conditions. The largest reductions at Stolb (19.0%) are projected by Group 4.

DISCUSSION

Model performance

This study expands research into the impacts of climate change on river discharge within the Arctic (e.g. Peterson *et al.* 2002; Arnell 2005) including, in comparison to other studies of the Lena (Ye *et al.* 2003), extending the geographical range downstream to Stolb.

Model performance for the baseline period was classified as at least 'very good', and in some cases 'excellent'. It was comparable to, and in some instances better than, other models of the Lena and similar basins (e.g. Gosling *et al.* 2017; Veldkamp *et al.* 2018). Model performance was relatively weaker at Vilui possibly due to a lack of information regarding the reservoir and thus its exclusion. Similar issues have been experienced elsewhere (Ho *et al.* 2016). Whilst performance for the validation period based on NSE was, in most cases, at least 'very good', discharges were notably underestimated, especially downstream. As previously stated, it is possible that this relates to a decline in how well the data used to force the model represent the basin's climate. Gridded CRU TS4.01 data are produced through interpolation of observations from meteorological stations (Harris *et al.* 2014). However, Arctic climatic observations are fraught with uncertainties due to sparse station networks, biases in measurements and changes in measurement methods (Rawlins *et al.* 2006). Within the Russian Arctic both the instruments used to measure precipitation and the frequency of observations have changed over time. There is also

potential for underestimation of precipitation due to difficulties in measuring snow, especially during windy winter conditions (Groisman *et al.* 1991). This could explain underestimated discharges at the most northern stations since unrealistically low winter snowfall will limit the volume of simulated spring meltwater. A mismatch between increasing Arctic discharge and declining or plateaued precipitation has been attributed to the closure of multiple meteorological stations in the late 20th Century (Groisman *et al.* 1991). Many high elevation stations were lost and thus interpolation is based on stations at lower elevations with potentially less precipitation (Wang *et al.* 2016). Poor model performance for the latter validation period supports the argument that these problems were particularly acute towards the end of the last century.

Projected hydrometeorological changes within the Lena Basin

Results suggest relatively small inter-GCM variability in projected temperatures across the Lena. Inter-GCM variability is larger for precipitation and PET with the range of change being slightly greater for precipitation, replicating results from other similar studies (Ho *et al.* 2016; Thompson *et al.* 2017a).

In general, model results suggest that discharge of the Lena River and its main tributaries will increase. This echoes findings of other studies that have highlighted increasing Arctic river flows (Peterson *et al.* 2002) and those that project future increases (Arnell, 2005; Gosling *et al.* 2011; 2017; Hattermann *et al.* 2017). The shift towards earlier snowmelt floods has been reported in Siberia and throughout the Arctic (e.g. Overeem and Syvitski, 2010; Vihma *et al.* 2016). Projected increases in winter precipitation, and hence deeper snow pack, will also contribute to higher spring discharges (Ye *et al.* 2004). The dominance of steeper recessions following the annual peak replicates results from Woo *et al.* (2008) that were attributed to increases in PET in excess of gains in precipitation. Although increased discharges dominate scenario results, the changes vary considerably in magnitude. This uncertainty could be constrained using GCM weightings (e.g. Maxino *et al.* 2008) following the approach of Krysanova *et al.* (2018) who recommend assessing models based on their performance, then weighting or excluding them as appropriate. This could reduce the number of GCM groups and therefore the number of scenarios and subsequent uncertainty. Nonetheless, utilising this approach introduces questions

322 regarding model exclusion, weight complexity and their derivation (Zaherpour *et al.* 2019), which
323 potentially adds further uncertainty.

324 In common with similar studies (e.g. Arnell 2005; Thompson *et al.* 2013), potential changes in vegetation
325 or anthropogenic interventions were not explicitly considered. Vegetation will shift northward with
326 altered climate regimes (Vihma *et al.* 2016) with potential hydrological feedbacks (Arnell 2005). The
327 omission of such features will have hydrological implications for processes such as PET, interception
328 and infiltration. The incorporation of future land use projections, such as those used within the Inter-
329 Sectoral Impact Model Intercomparison Project (ISIMIP2b; Frieler *et al.* 2017), which themselves are
330 impacted by climatic and socio-economic drivers, would enable these impacts to be simulated.
331 Permafrost melt, which as previously noted was not included in this and other models used to assess
332 climate change impacts on the Lena and other similar basins (e.g. Gosling *et al.* 2017; Veldkamp *et al.*
333 2018), would also have hydrological implications including enhanced infiltration that may contribute to
334 increasing groundwater contributions to river flow (Walvoord and Striegl 2007; Vihma *et al.* 2016). In
335 contrast, continued melting may enhance vertical flow paths enough that increased infiltration reduces
336 the volume of water reaching the river (Walvoord and Kurylyk 2016). These changes may be most
337 significant in higher latitude sub-catchments due to the greater projected temperature increases
338 (Gautier *et al.* 2018).

339 This study focussed on GCM-related uncertainty in future hydrometeorological conditions within the
340 Lena Basin and did not consider hydrological model-related uncertainty. This could be investigated by
341 simulating the same climate change scenarios with a number of hydrological models of the Lena using
342 alternative model codes to MIKE SHE, the different process descriptions available within MIKE SHE or
343 alternative parameterisations and spatial distributions of model input data (e.g. Thompson *et al.* 2013,
344 2014, Robinson 2018). Whilst the overall fraction of uncertainty within hydrological impact studies of
345 climate change that is attributable to different hydrological models has been shown to be smaller than
346 that due to different GCMs (e.g. Krysanova *et al.* 2017), choice of hydrological model may not be
347 insignificant where processes are implemented uniquely in different models (Hattermann *et al.* 2018).
348 Snowmelt schemes, for example, include degree-day methods as used here or more complex energy
349 balance approaches (Pohl *et al.* 2005; Corripio and López-Moreno, 2017). Given the significance of snow

accumulation and melt within the Lena, these different methods could simulate variable responses to the same climate change scenario.

Implications for the Atlantic Meridional Overturning Circulation

Increases in mean discharge at Stolb dominate scenario results (10 of 12 GCM groups). Projections range between -5.3% (840 m^3s^{-1}) and +21.7% (3,440 m^3s^{-1}) with the group ensemble mean projecting an increase of 9.2% (1,458 m^3s^{-1}). These results can be used to provide estimates of potential changes in Eurasian runoff to the Arctic Ocean. The Lena, Yenisei and Ob contribute approximately 45% (~46,700 m^3s^{-1}) of the mean annual runoff to the Arctic (Ye *et al.* 2004). Changes in these inflows can be established if percentage changes for Stolb are applied to the downstream gauging station of each river (Igarka and Salekhard for Yenisei and Ob, respectively; R-Arctic.Net). These estimates assume regionally homogeneous climatic changes, the same hydrological responses to these changes within the Yenisei and Ob basins, and exclude future anthropogenic impacts. Whilst it is recognised that this is a simplification, the approach does enable an initial assessment of climate change driven modifications to Eurasian runoff to the Arctic for each of the 12 GCM groups. Increases of between 1,729 m^3s^{-1} and 10,146 m^3s^{-1} (1.7–10.1mSv) (1Sv = 1000mSv = 10^6 m^3s^{-1}) are projected for ten groups (declines of 0.8m–2.5mSv for two) and the group ensemble mean (Figure 6).

Peterson *et al.* (2002) suggested that an additional freshwater flux of between 60–150mSv would inhibit NADW formation. The changes summarised in Figure 6 are far below these values. However, sustained enhanced fluxes of 5-100mSv could weaken convection (Schulz *et al.* 2007; Yang *et al.* 2016). Four of the GCM groups (1, 3, 5 and 9) project fluxes that cross the minimum threshold with projections for Group 10 coming close (Figure 6). Climate-induced changes in Eurasian river discharge under RCP4.5 may, therefore, produce freshwater fluxes capable of weakening AMOC. This extends the analysis of Shu *et al.* (2017), who found that enhanced runoff from all Arctic rivers under RCP8.5 could weaken AMOC, by suggesting that such weakening may occur under a broader range of future climate conditions. Additionally, as Lena discharge shows increases with temperature (Gosling *et al.* 2017), it is likely that under the higher temperatures projected by RCP6.0 and RCP8.5, discharge may increase further, thus causing a more substantial weakening of AMOC. Therefore, whilst AMOC collapse may be improbable

during the 21st Century, it may be more likely in the future. Furthermore, the increases projected herein will be coupled with warmer temperatures (Thornalley *et al.* 2013), likely increased North American Arctic discharges (e.g. Arnell 2005; Shu *et al.* 2017), greater precipitation, and meltwater from the Greenland ice sheet (Vihma *et al.* 2016), which will all also act to reduce convection. These changes will increase the potential for weakening of the AMOC that will have important implications for global climate.

CONCLUSION

A MIKE SHE/MIKE 11 model was used to investigate climate change impacts on discharge within the Lena River Basin for 12 genealogical-based GCM groups and the RCP4.5 scenario in 2071–2100. All groups projected basin-wide increases in precipitation, temperature and PET. However, the magnitudes of changes varied. Increases in mean annual discharge dominate with declines restricted to two groups. Seasonal shifts in the timing of snowmelt were simulated due to increases in temperature and precipitation during winter and spring. The application of projected changes to the three major Eurasian rivers suggests that AMOC weakening could potentially occur should enhanced freshwater inputs be sustained. When augmented by increases in other freshwater sources, and combined with higher temperature more groups may cross the threshold, increasing the likelihood of AMOC weakening by the end of the 21st Century. Eurasian rivers alone could, therefore, play a significant role in altering this component of the Earth's climate system.

Acknowledgements

We thank two anonymous reviewers for their valuable comments and suggestions on earlier drafts of the manuscript.

References

Allen, R., Pereira, L. Raes, D. and Smith, M. 1998 *Crop evapotranspiration – guidelines for computing crop water requirements,* Food and Agriculture Organisation, Rome.

Andersen, J., Refsgaard, J.C. and Jensen, K.H. 2001 Distributed hydrological modelling of the Senegal River Basin – model construction and validation. *Journal of Hydrology*, **247**, 200-214.

Arnell, N.W. 2005 Implications of climate change for freshwater inflows to the Arctic Ocean. *Geophysical Research Letters*, **27**, 1183-1186.

Atwell, B., Kriedemann, P. and Turnbull, C. 1999 *Plants in action: adaptations in nature, performance in cultivation*, MacMillan Education Australia, South Yarra.

Berezovskaya, S., Yang, D. and Hinzman, L. 2005 Long-term annual water balance analysis of the Lena River. *Global and Planetary Change*, **48**, 84-95.

Broecker, W.S., Peteet, D.M. and Rind, D. 1985 Does the ocean-atmosphere system have more than one stable mode of operation? *Nature*, **315**, 21-26.

Buckley, M.W. and Marshall, J. 2016 Observations, inferences, and mechanisms of the Atlantic Meridional Overturning Circulation: A review. *Reviews of Geophysics,* **54**, 5-63.

Clark, P.U., Pisias, N.G., Stocker, T.F. and Weaver, A.J. 2002 The role of the thermohaline circulation in abrupt climate change. *Nature,* **415**, 863-869.

Corripio, J.G. and López-Moreno, J.I. 2017 Analysis and predictability of the hydrological response of mountain catchments to heavy rain on snow events: A case study in the Spanish Pyrenees. *Hydrology,* **4**, 20.

Dzhamalov, R., Krichevets, G. and Safronova, T. 2012 Current changes in water resources in Lena River basin. *Water Resources*, **39**, 147-160.

Frieler, K.P., Lange, S.A., Piontek, F.D., Reyer, C.P.O.P., Schewe, J.K., Warszawski, L.N., Zhao, F.F., Geiger, T., Mengel, M., Ostberg, S., Popp, A., Stevanovic, M., Volkholz, J., Hattermann, F., Huber, V., Jägermeyr, J., Krysanova, V., Mouratiadou, I., Bodirsky, B.L., Lotze-Campen, H., Thonicke, K., Chini, L., Hurtt, G., Sahajpal, R., Denvil, S., Emanuel, K., Halladay, K., Burke, E., Betts, R.A., Jones, C.D., Murakami, D., Riva, R., Suzuki, T., Ciais, P., Vautard, R., Ebi, K., Eddy, T.D., Tittensor, D.P., Lotze, H.K., Elliott, J., Deryng, D., Galbraith, E., Gosling, S.N., Hickler, T., Hof, C., Schmied, H.M., Biber, M.F., Hinkel, J., Marcé, R., Pierson, D., Van Vliet, M., Frolking, S., Tian, H. and Yamagata, Y. 2017 Assessing the Impacts of 1.5°C Global Warming - Simulation Protocol of the Inter-Sectoral Impact Model Intercomparison Project (ISIMIP2b), *Geoscientific Model Development,* **10**, 4321-4345.

Gautier, E., Dépret, T., Costard, F., Virmoux, C., Deforov, A., Grancher, D., Konstantinov P. and Brunstein D. 2018 Going with the flow: Hydrologic response of the middle Lena River (Siberia) to the climate variability and change. *Journal of Hydrology*, **557**, 475-488.

Gelfan, A., Gustafsson, D., Motovilov, Y., Arheimer, B., Kalugin, A., Krylenko I. and Lavrenov, A. 2017 Climate change impact on the water regime of two great Arctic rivers: modelling and uncertainty issues. *Climatic Change*, **141**, 499-515.

Gosling, S.N. 2013 The likelihood and potential impact of future change in the large-scale climate-earth system on ecosystem services, *Environmental Science and Policy*, **27**, 15-31.

Gosling, S.N., Taylor, R.G., Arnell N.W. and Todd M.C. 2011 A comparative analysis of projected impacts of climate change on river runoff from global and catchment-scale hydrological models. *Hydrology and Earth System Sciences*, **15**, 279-294.

Gosling, S.N., Zaherpour, J., Mount, N.J., Hattermann, F.F., Dankers, R., Arheimer, B., Breuer, L., Ding, J., Haddeland, I., Kumar, R., Kundu, D., Liu, J., Van Griensven, A., Veldkamp, T.I.E., Vetter, T., Wang, X. and Zhang, X. 2017 A comparison of changes in river runoff from multiple global and catchment-scale hydrological models under global warming scenarios of 1°C, 2°C and 3°C. *Climatic Change*, **141**, 577-595.

Groisman P., Koknaeva, V., Belokrylova, T. and Karl, T. 1991 Overcoming biases of precipitation measurement: a history of the USSR experience. *Bulletin of the American Meteorological Society*, **72**, 1725-1733.

Hargreaves, G.H. and Samani, Z.A. 1985 Reference crop evapotranspiration from temperature. *Applied Engineering in Agriculture*, **1**, 96-99.

Harris, I., Jones, P., Osborn, T., and Lister, D. 2014 Updated high-resolution grids of monthly climatic observations – the CRU TS3.10 Dataset. *International Journal of Climatology*, **34**, 623-642.

Hattermann, F.F., Krysanova, V., Gosling, S.N., Dankers, R., Daggupati, P., Donnelly, C., Flörke, M., Huang, S., Motovilov, Y., Buda, S., Yang, T., Müller, C., Leng, G., Tang, Q., Portmann, F.T., Hagemann, S., Gerten, D., Wada, Y., Masaki, Y., Alemayehu, T., Satoh Y. and Samaneigo, L. 2017 Cross-scale intercomparison of climate change impacts simulated by regional and global hydrological models in eleven large river basins, *Climatic Change*, **141**, 561-576.

Hattermann, F.F., Vetter, T., Breuer, L., Su, B., Daggupati, P., Donnelly, C., Fekete, B., Flörke, F., Gosling, S.N., Hoffmann, P., Liersch, S., Masaki, Y., Motovolov, Y., Müller, C., Samaniego, L., Stacke, T., Wada, Y., Yang T., and Krysnaova, V. 2018 Sources of uncertainty in hydrological climate impact assessment: a cross-scale study. *Environmental Research Letters*, **13**, 015006.

Hawkins, E., Smith, R.S., Allison, L.C., Gregory, J.M., Woollings, T.J., Pohlmann, H., and De Cuevas, B. 2011 Bistability of the Atlantic overturning circulation in a global climate model and links to ocean freshwater transport. *Geophysical Research Letters,* **38**, L10605.

Henriksen, H.J., Troldborg, L., Nyegaard, P., Sonnenborg, T.O., Refsgaard, J.C. and Madsen, B. 2003 Methodology for construction, calibration and validation of a national hydrological model for Denmark. *Journal of Hydrology*, **280**, 52-71.

Ho, J.T., Thompson, J.R. and Brierley, C. 2016 Projections of hydrology in the Tocantins-Araguaia Basin, Brazil: uncertainty assessment using the CMIP5 ensemble. *Hydrological Sciences Journal*, **61**, 551-567.

Holmes, R.M., McClelland, J.W., Peterson, B.J., Tank, S.E., Bulygina, E., Eglinton, T.I., Gordeev, V.V., Gurtovaya, T.Y., Raymond, P.A., Repeta, D.J., Staples, R., Striegl, R.G., Zhulidov A.V. and Zimov, S.A. 2012 Seasonal and annual fluxes of nutrients and organic matter from large rivers to the Arctic Ocean and Surrounding seas. *Estuaries and Coasts*, **35**, 369-382.

Immerzeel, W., Pellicciotti, F. and Shrestha, A. 2012 Glaciers as a Proxy to Quantify the Spatial Distribution of Precipitation in the Hunza Basin. *Mountain Research and Development*, **32**, 30-38.

Ji, X. and Luo, Y. 2013 The influence of precipitation and temperature input schemes on hydrological simulations of a snow and glacier melt dominated basin in Northwest China. *Hydrology and Earth System Sciences*, **10**, 807-853.

Keller, K., Tan, K., Morel, F.M.M. and Bradford, D.F. 2000. Preserving the Ocean Circulation: Implications for Climate Policy. *Climatic Change,* **47**, 17-43.

Kirtman, B., Power, S.B., Adedoyin, J.A., Boer, G.J., Bojariu, R., Camilloni, I., Doblas-Reyes, F.J., Fiore, A.M., Kimoto, M, Meehl, G.A., Prather, M., Sarr, A., Schär, C., Sutton, R., van Oldenborgh, G.J., Vecchi G. and Wang, H.J. 2013. Near-term climate change: projections and predictability. In: *Climate Change 2013: The Physical Science Basis. Contribution of Working Group I to the Fifth Assessment Report of the Intergovernmental Panel on Climate Change,* T.F. Stocker, D. Qin, G.-K. Plattner, M. Tignor, S.K. Allen, J. Boschung, A. Nauels, Y. Xia, V. Bex and P.M. Midgley (eds), Cambridge University Press, Cambridge, pp. 953-1028.

Köhler, P., Joos, F., Gerber, S. and Knutti, R. 2005. Simulated changes in vegetation distribution, land carbon storage, and atmospheric CO2 in response to a collapse of the North Atlantic thermohaline circulation. *Climate Dynamics*, **25**, 689-708.

Kingston, D.G., Thompson, J.R. and Kite, G. 2011. Uncertainty in climate change projections of discharge for the Mekong River Basin. *Hydrology and Earth System Sciences* **15**, 1459-1471.

Krysanova, V., Donnelly, C., Gelfan, A., Gerten, D., Arheimer, B., Hattermann, F. and Kundzewicz, Z.W. 2018. How the performance of hydrological models relates to credibility of projections under climate change. *Hydrological Sciences Journal*, **63**, 696-720.

Krysanova, V., Vetter, T., Eisner, S., Huang, S., Pechlivanidis, I., Strauch, M., Gelfan, A., Kumar, R., Aich, V., Arheimer, B. and Chamorro, A. 2017 Intercomparison of regional-scale hydrological models and climate

change impacts projected for 12 large river basins worldwide—a synthesis. *Environmental Research Letters*, **12**, 105002.

Kuhlbrodt, T., Rahmstorf, S., Zickfeld, K., Vikebø, F., Sundby, S., Hofmann, M., Link, P., Bondeau, A., Cramer, W. and Jaeger, C. 2009. An Integrated Assessment of changes in the thermohaline circulation. *Climatic Change*, **96**, 489–537.

Liu, B. and Yang, D. 2011 Siberian Lena River heat flow regime and change. *Cold Region Hydrology in a Changing Climate*, **346**, 71-76.

Manabe, S. and Stouffer, R.J. 1988 Two stable equilibria of a coupled ocean-atmosphere model. *Journal of Climate,* **1**, 871-884.

Maxino, C.C., Mcavaney, B.J., Pitman, A.J. and Perkins, S.E. 2008 Ranking the AR4 climate models over the Murray-Darling Basin using simulated maximum temperature, minimum temperature and precipitation. *International Journal of Climatology*, **28**, 1097-1112.

Overeem, I. and Syvitski, J.P.M. 2010 Shifting discharge peaks in arctic rivers, 1977–2007. *Geografiska Annaler: Series A, Physical Geography*, **92**, 285-296.

Overland, J.E., Wang, M., Walsh, J.E. and Stroeve, J.C. 2013 Future Arctic climate changes: Adaptation and mitigation time scales. *Earth's Future*, **2**, 68-74.

Peterson B.J., Holmes, R.M, McClelland, J.W., Vörösmarty, C.J., Lammers, R.B., Shiklomanov, A.I., Shiklomanov I.A. and Rahmstorf, S. 2002 Increasing River Discharge to the Arctic Ocean. *Science,* **298**, 2171-2173.

Pirtle, Z., Meyer, R. and Hamilton, A. 2010 What does it mean when climate models agree? A case for assessing independence among general circulation models. *Environmental Science and Policy,* **13**, 351-361.

Pohl, S., Davison, B., Marsh, P. and Pietroniro, A. 2005. Modelling spatially distributed snowmelt and meltwater runoff in a small Arctic catchment with a hydrology land-surface scheme (WATCLASS), *Atmosphere-Ocean,* **43**, 193-211.

Rawlins, M.A., Willmott, C.J., Shiklomanov, A., Linder, E., Frolking, S., Lammers, R.B. and Vörösmarty, C.J. 2006 Evaluation of trends in derived snowfall and rainfall across Eurasia and linkages with discharge to the Arctic Ocean. *Geophysical Research Letters*, **33**, L07403.

Refsgaard, J.C., Storm, B. and Clausen, T., 2010 Système Hydrologique Europeén (SHE): review and perspectives after 30 years development in distributed physically-based hydrological modelling. *Hydrology Research* **41**, 355–377.

Robinson, A.J. 2018 *Uncertainty in hydrological scenario modelling: An investigation using the Mekong River Basin, SE Asia*. PhD Thesis, UCL, London.

Schulz, M., Prange, M. and Klocker, A. 2007 Low-frequency oscillations of the Atlantic Ocean meridional overturning circulation in a coupled climate model. *Climate of the Past*, **3**, 97-107.

Shiklomanov, I.A., Shiklomanov, A.I., Lammers, R.B., Peterson, B.J. and Vörösmarty, C.J. 2000 The dynamics of river water inflow to the Arctic Ocean. In: *The Freshwater Budget of the Arctic Ocean: Proceedings of the NATO Advanced Research Workshop*, E.L. Lewis, E.P. Jones and P. Lemke (eds), Kluwer, Dordrecht, pp. 281–296.

Shu, Q., Qiao, F., Song Z. and Xiao, B. 2017 Effect of increasing Arctic river runoff on the Atlantic meridional overturning circulation: a model study. *Acta Oceanologica Sinica*, **36**, 59-65.

Thompson, J.R., Crawley, A. and Kingston, D.G. 2017a Future river flows and flood extent in the Upper Niger and Inner Niger Delta: GCM-related uncertainty using the CMIP5 ensemble. *Hydrological Sciences Journal*, **62**, 2239-2265.

Thompson, J.R., Iravani, H., Clilverd, H.M., Sayer, C.D., Heppell, C.M., and Axmacher, J.C. 2017b Simulation of the hydrological impacts of climate change on a restored floodplain. *Hydrological Sciences Journal*, **62**, 2482-2510.

Thompson, J.R., Green, A.J. and Kingston, D.J. 2014 Potential evapotranspiration-related uncertainty in climate change impacts on river flow: An assessment for the Mekong River. *Journal of Hydrology*, **510**, 259-279.

Thompson, J.R., Green, A.J. and Kingston, D.J. and Gosling, S.N. 2013 Assessment of uncertainty in river flow projections for the Mekong River using multiple GCMs and hydrological models. *Journal of Hydrology*, **486**, 1-30.

Thompson, J.R., Refstrup-Sørenson, H., Gavin, H. and Refsgaard, A. 2004 Application of the coupled MIKE SHE / MIKE 11 modelling system to a lowland wet grassland in Southeast England. *Journal of Hydrology*, **293**, 151-179.

Thornalley, D.J.R., Blaschek, M., Davies, F.J., Praetorius, S., Oppo, D.W., McManus, J.F., Hall, I.R., Kleiven, H., Renssen, H. and McCave, I.N. 2013 Long-term variations in Iceland-Scotland overflow strength in the Holocene. *Climate of the Past*, **9**, 2073-2084.

UNFCCC 2015 *Adoption of the Paris Agreement, 21st Conference of the Parties*. United Nations, Paris.

Veldkamp, T.I.E., Zhao, F., Ward, P.J., de Moel, H., Aerts, J.C.J.H., Muller Schmied, H., Portmann, F.T., Masaki, Y., Pokhrel, Y., Liu, X., Satoh, Y., Gerten, D., Gosling, S.N., Zaherpour, J. and Wada, Y. 2018 Human impact parameterisations in global hydrological models improve estimates of monthly discharges and hydrological extremes: a multi-model validation study. *Environmental Research Letters*, **13**, 055008.

Vellinga, M., and Wood, R.A. 2008. Impacts of thermohaline circulation shutdown in the twenty-first century. *Climatic Change,* **91,** 43-63.

566 Vihma, T., Screen, J., Tjerström, M., Newton, B., Zhang, X., Popova, V., Deser, C., Holland, M. and Prowse,
567 T. 2016 The atmospheric role in the Arctic water cycle: A review on processes, past and future changes,
568 and their impacts. *Journal of Geophysical Research*, **121**, 586-620.

569 Walvoord, M.A. and Kurylyk, B.L. 2016 Hydrologic impacts of thawing permafrost – a review. *Vadose*
570 *Zone Journal*, **15**, 1-20.

571 Walvoord, M.A. and Striegl, R.G. 2007 Increased groundwater to stream discharge from permafrost
572 thawing in the Yukon River basin: potential impacts on lateral export of carbon and nitrogen,
573 *Geophysical Research Letters*, **34**, 1-6.

574 Wang, Q., Fan, X. and Wang, M. 2016 Evidence of high-elevation amplification versus Arctic
575 amplification. *Scientific Reports*, **6**, 19219.

576 Woo, M.-K., Thorne, R., Szeto, K. and Yang, D. 2008 Streamflow Hydrology in the Boreal Region under
577 the Influences of Climate and Human Interference. *Philosophical Transactions: Biological Sciences,* **363**,
578 2251-2260.

579 Yang, Q., Dixon, T., Myers, P., Bonin, J., Chambers D. and Van Den Broeke, M. 2016 Recent increases in
580 Arctic freshwater flux affects Labrador Sea convection and Atlantic overturning circulation. *Nature*
581 *Communications*, **7**, 1-7.

582 Ye, B., Yang, D. and Kane, D.L. 2003 Changes in Lena River streamflow hydrology: Human impacts versus
583 natural variations. *Water Resources Research*, **39**, 1200.

584 Ye, H., Yang, D., Zhang, T., Shang, X., Ladochy S. and Ellison, M. 2004 The impact of Climatic Conditions
585 on Seasonal River Discharges in Siberia. J*ournal of Hydrometeorology*, **5**, 286-295.

586 Zaherpour, J., Mount, N., Gosling, S.N., Dankers, R., Eisner, S., Gerten, D., Liu, X., Masaki, Y., Schmied, H.M.,
587 Tong Q. and Wada, Y. 2019 Exploring the value of machine learning for weighted multi-model
588 combination of an ensemble of global hydrological models. *Environmental Modelling and Software*, **114**,
589 112-128.

590 **Tables**

591 *Table 1. Data used in the MIKE SHE/MIKE 11 model of the Lena River Basin*
592

Component within model	Data source and derivation	Use within the MIKE SHE/MIKE 11 model
Basin area	Obtained using the USGS GTOPO30 DEM[1]	Defined the model domain within MIKE SHE and specified as a shapefile.
Topography	Values extracted from the USGS GTOPO-30 DEM	Defined the topography within MIKE SHE. Specified as a grid file.
Sub-catchments	The USGS GTOPO-30 DEM, R-ArcticNET[2] gauging station locations and major tributaries.	Defined five main sub-catchments within MIKE SHE. Specified as a shapefile. Also defined the linear reservoir sub-catchments and baseflow sub-catchments. A grid file defined the locations of the smaller 19 meteorological sub-catchments, which allowed the spatial distribution of climatic variables. Within these areas, parameters were adjusted during model calibration.
Land use	USGS 1km Global Land Cover Characterisation data[3]	Defined the spatial distribution of land use within the Lena River Basin. 29 original classes were re-classified into nine classes. Specified as a grid file.
Vegetation properties: Root Depth and Leaf Area Index	Values from the literature (Arnell, 2005)	A root depth was defined for each land cover class. This value describes the depth of the zone from with evapotranspiration can occur. These were constant for each land cover classes. Leaf area index describes the ratio of the leaf area to the ground area.
River network	Using the USGS GTOPO-30, the river network was identified using ArcMAP Hydrology Tools.	A shapefile was specified in MIKE 11. It was then manually digitized to define the river network.
Cross-sections	Identified and measured using Google Earth Pro. Elevations were extracted from the basin DEM.	Defined channel cross-sections within MIKE 11. Each channel width was assigned a stream order. Elevations were assigned to each cross-section.
Overland Flow: Manning Number	Values from the literature using the approach of Thompson *et al.* (2013).	This was spatially distributed throughout the catchment based on the overlying vegetation. Specified as a grid file. Defined the rate at which overland flow is routed to channels.
Unsaturated Zone: Soil properties	FAO Digital Soil Map of the World[4]. Using ArcMap, the basin was separated into three main soil classes. Values from the literature (Atwell *et al.* 1999).	Defined for the water content at saturation, water content at field capacity, water content at wilting point and saturated hydraulic conductivity within the basin.

593 *1. lta.cr.usgs.gov/GTOPO30*
594 *2. www.r-arcticnet.sr.unh.edu/v4.0/index.html*
595 *3. lta.cr.usgs.gov/GLCC*
596 *4. www.fao.org/soils-portal/soil-survey/soil-maps-and-databases*
597

598

599 *Table 2. The CMIP5 GCMs and their grouping by genealogy.*

No	GCM	Institution	GCM Group
1	ACCESS1.0	Commonwealth Scientific and Industrial Research Organisation (CSIRO) and	10
2	ACCESS1.3	Bureau of Meteorology (BOM), Australia	10
3	BCC-CSM1.1	Beijing Climate Center, China Meteorological Administration	12
4	BCC-CSM1.1(m)		12
5	BNU-ESM	College of Global Change and Earth System Science, Beijing Normal University	12
6	CanESM2	Canadian Centre for Climate Modelling and Analysis	1
7	CCSM4	National Center for Atmospheric Research	12
8	CESM1(BGC)	Community Earth System Model Contributors	12
9	CESM1(CAM5)		12
10	CMCC-CM	Centro Euro-Mediterraneo per I Cambiamenti Climatici	11
11	CMCC-CMS		11
12	CNRM-CM5	Centre National de Recherches Météorologiques/ Centre Européen de Recherche et Formation Avancée en Calcul Scientifique	11
13	CSIRO-Mk3.6.0	Commonwealth Scientific and Industrial Research Organisation in collaboration with Queensland Climate Change Centre of Excellence	2
14	EC-EARTH	EC-Earth consortium	11
15	FGOALS-g2	LASG, Institute of Atmospheric Physics, Chinese Academy of Sciences	3
16	FIO-ESM	The First Institute of Oceanography, SOA, China	12
17	GFDL-CM3	NOAA Geophysical Fluid Dynamics Laboratory	6
18	GFDL-ESM2G		6
19	GFDL-ESM2M		6
20	GISS-E2-H p1	NASA Goddard Institute for Space Studies	7
21	GISS-E2-H p2		7
22	GISS-E2-H p3		7
23	GISS-E2-H-CC		7
24	GISS-E2-R p1		7
25	GISS-E2-R p2		7
26	GISS-E2-R p3		7
27	GISS-E2-R-CC		7
28	HadGEM2-AO	Met Office Hadley Centre (additional HadGEM2-ES realizations contributed by	10
29	HadGEM2-CC	Instituto Nacional de Pesquisas Espaciais)	10
30	Had-GEM2-ES		10
31	INM-CM4	Institute for Numerical Mathematics	4
32	IPSL-CM5A-LR	Institut Pierre-Simon Laplace	8
33	IPSL-CM5A-MR		8
34	IPSL-CM5B-LR		8
35	MIROC5	Atmosphere and Ocean Research Institute (The University of Tokyo), National Institute for Environmental Studies, and Japan Agency for Marine-Earth Science and Technology	9
36	MIROC-ESM	Japan Agency for Marine-Earth Science and Technology, Atmosphere and Ocean	9
37	MIROC-ESM-CHEM	Research Institute (The University of Tokyo), and National Institute for Environmental Studies	9
38	MPI-ESM-LR	Max-Planck-Institut für Meteorologie (Max Planck Institute for Meteorology)	11
39	MPI-ESM-MR	Meteorological Research Institute	11
40	MRI-CGCM3		5
41	NorESM1-M	Norwegian Climate Centre	12

Genealogy-based GCM groups

No	Group name	Number of GCMs	No	Group name	Number of GCMs	No	Group name	Number of GCMs
1	CanESM2	1	5	MRI-CGCM3	1	9	MIROC	3
2	CSIRO-Mk3.6.0	1	6	GFDL	3	10	UKMO	5
3	FGOALS-g2	1	7	GISS	8	11	European	6
4	INM-CM4	1	8	IPSL	3	12	NCAR	8

600

Table 3. Model performance statistics and classification for the calibration (Cal, 1960-1979), baseline (1961-1990) and validation (Val, 1980-1999) periods. Model performance classification is based on Ho et al. (2016) and adapted from Henriksen et al. (2003).

Station	Period	Dv		NSE		r	
Tabaga	Cal	-3.27	✓✓✓✓✓	0.90	✓✓✓✓✓	0.95	✓✓✓✓✓
	Baseline	-3.87	✓✓✓✓✓	0.83	✓✓✓✓	0.95	✓✓✓✓✓
	Val	-10.00	✓✓✓	0.83	✓✓✓✓	0.93	✓✓✓✓
Aldan	Cal	8.14	✓✓✓✓	0.88	✓✓✓✓✓	0.95	✓✓✓✓✓
	Baseline	3.23	✓✓✓✓✓	0.83	✓✓✓✓	0.95	✓✓✓✓✓
	Val	-8.25	✓✓✓✓	0.79	✓✓✓✓	0.92	✓✓✓✓
Vilui	Cal	5.33	✓✓✓✓	0.82	✓✓✓✓	0.90	✓✓✓✓
	Baseline	-2.17	✓✓✓✓✓	0.66	✓✓✓✓	0.87	✓✓✓
	Val	-16.47	✓✓	0.49	✓✓	0.77	✓
Kusur	Cal	-5.03	✓✓✓✓	0.74	✓✓✓✓	0.87	✓✓✓
	Baseline	-7.87	✓✓✓✓	0.63	✓✓✓	0.88	✓✓✓
	Val	-12.70	✓✓✓	0.76	✓✓✓✓	0.92	✓✓✓✓
Stolb	Cal	5.69	✓✓✓✓	0.70	✓✓✓✓	0.83	✓✓
	Baseline	2.44	✓✓✓✓✓	0.61	✓✓✓	0.76	✓
	Val	-5.22	✓✓✓✓	0.80	✓✓✓✓	0.92	✓✓✓✓

Performance indicator	Excellent ✓✓✓✓✓	Very good ✓✓✓✓	Fair ✓✓✓	Poor ✓✓	Very poor ✓
Dv	< 5%	5–10%	10–20%	20–40%	>40%
NSE	>0.85	0.65–0.85	0.50–0.65	0.20–0.50	<0.20
r	≥0.95	0.90-0.94	0.85-0.89	0.80-0.84	<0.80

606 **Figures**

607

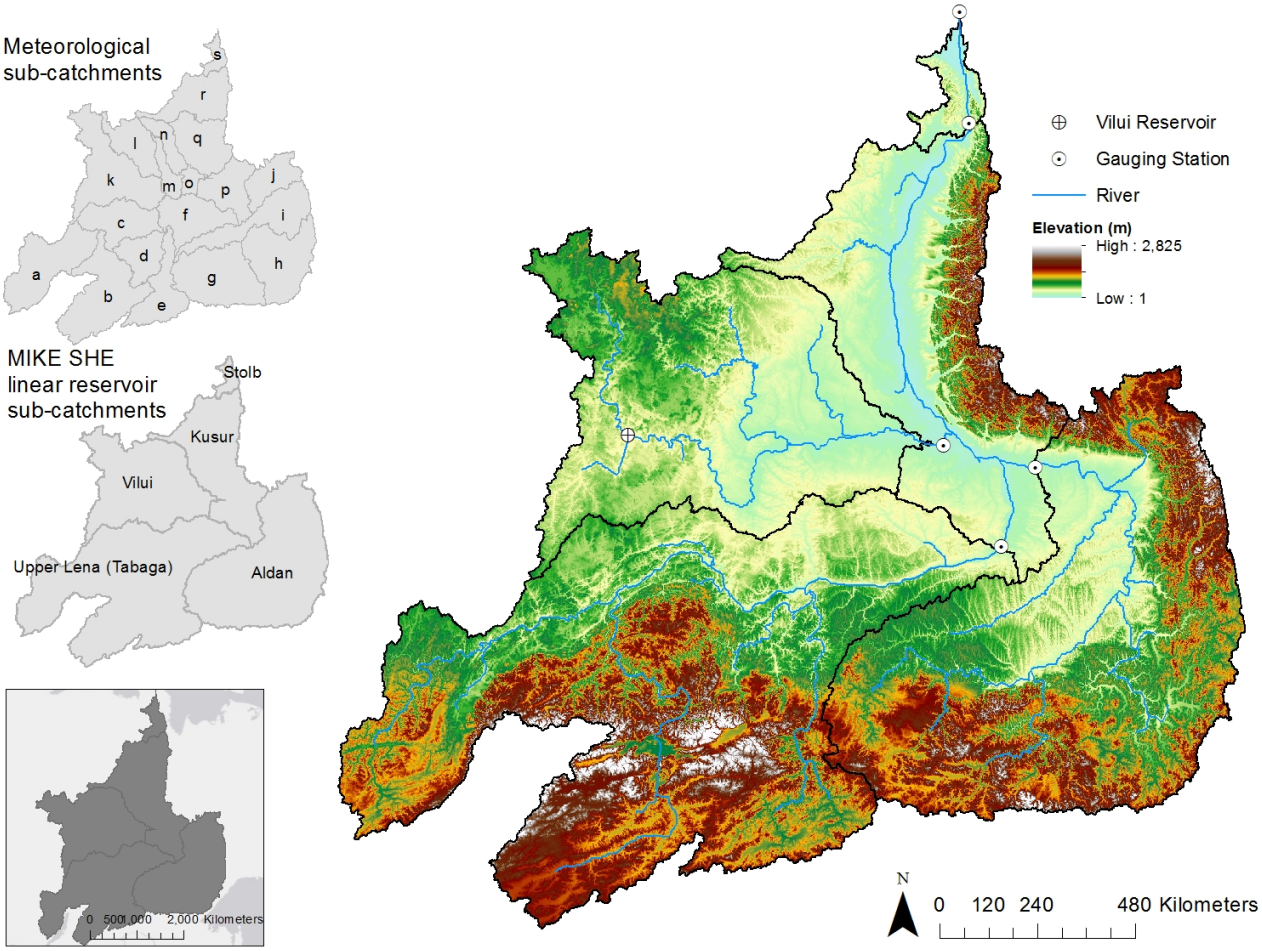

608
609
610 *Figure 1. The Lena River Basin including the locations of five gauging stations for which river discharge is*
611 *simulated and the sub-catchments used within the MIKE SHE model.*
612

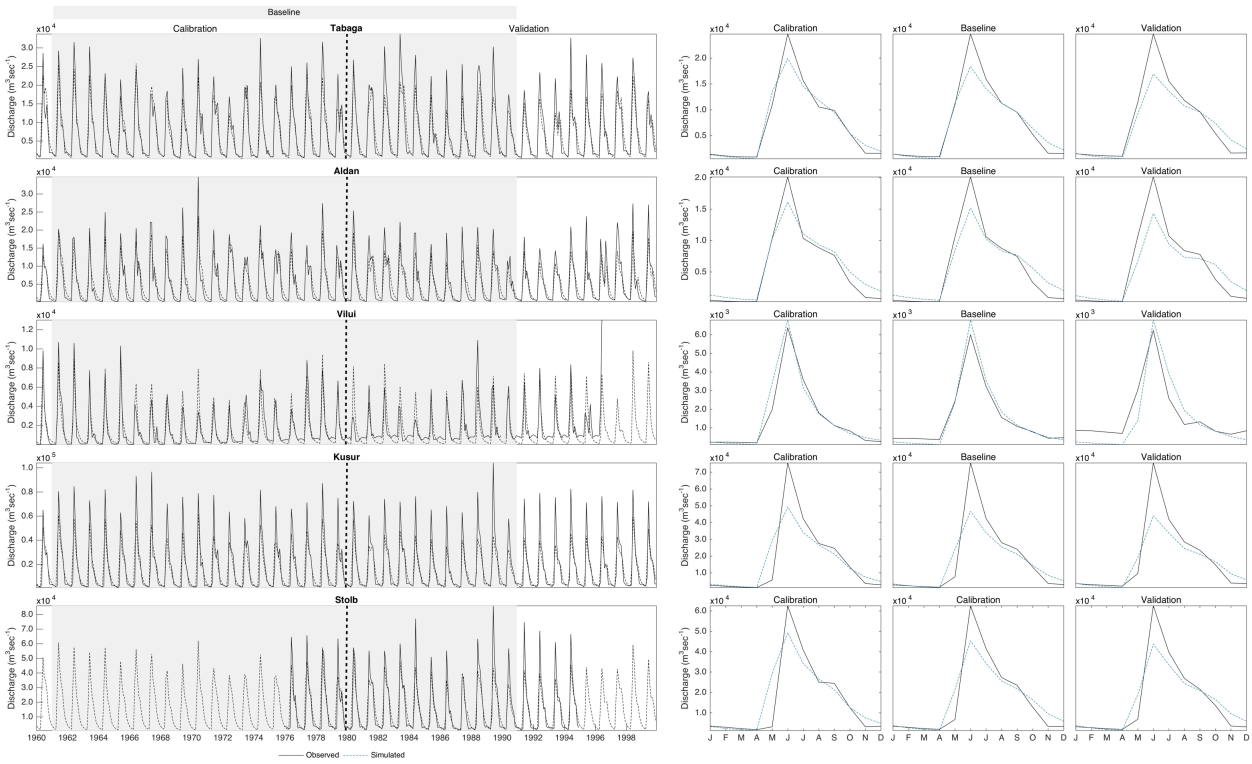

Figure 2. Observed and simulated mean monthly discharge and river regimes at the five gauging stations within the Lena River Basin for the calibration (1960–1979), baseline (1961–1990) and validation (1980–1999) periods. Note different y-axis scales.

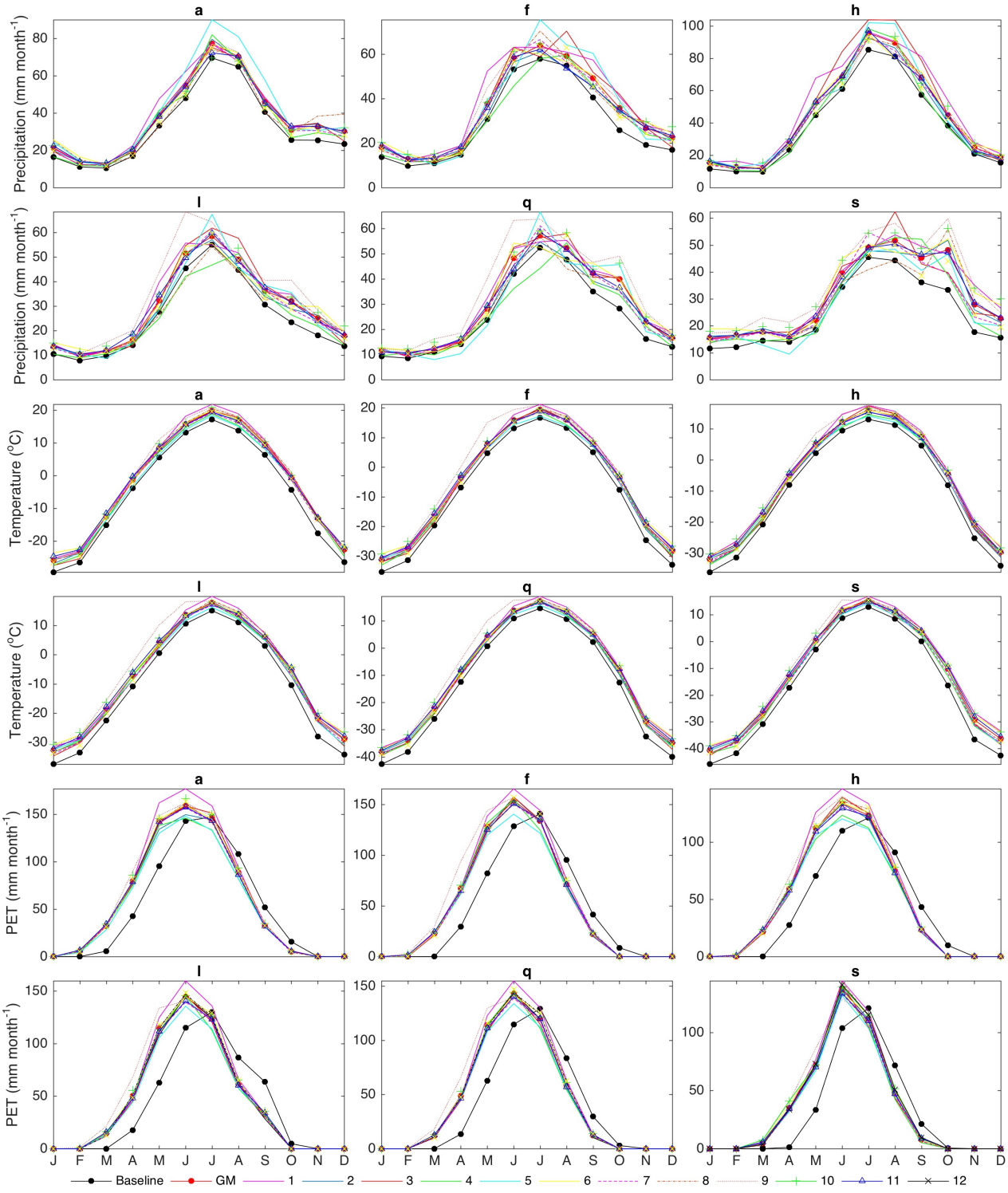

Figure 3. Mean monthly precipitation (precip.), temperature and PET in six representative sub-catchments in the Lena River Basin for the baseline, each GCM group and the group ensemble mean (GM). Note different y-axis scales.

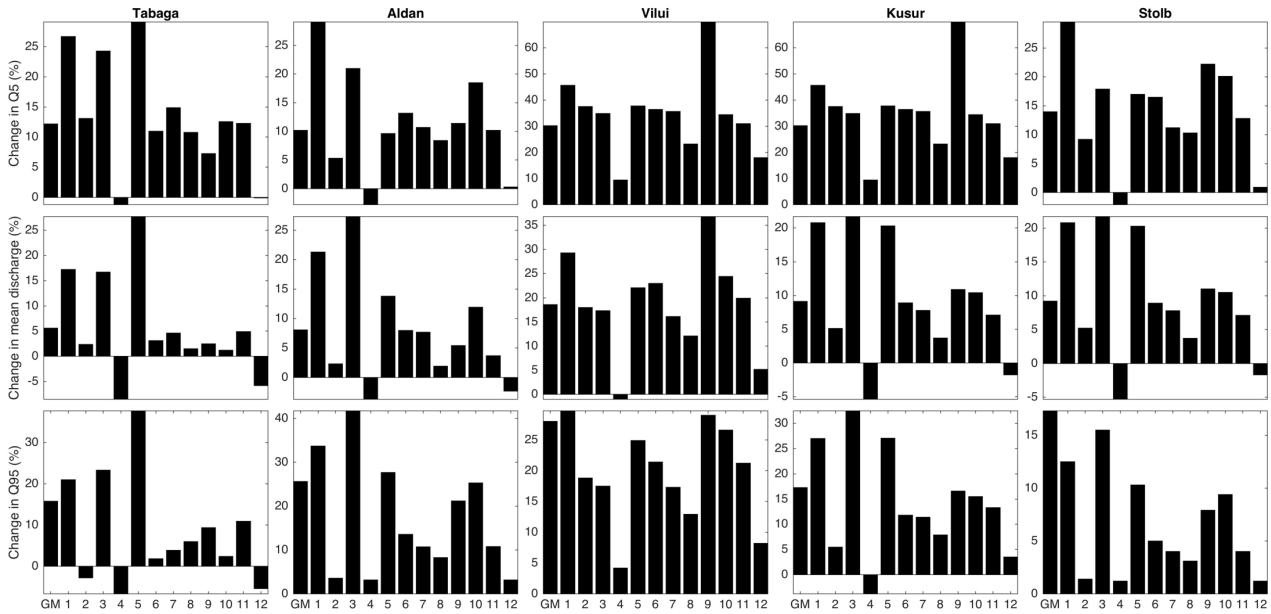

Figure 4. Percentage changes in mean discharge, high (Q5) and low (Q95) discharges for each gauging station in the Lena River Basin. Note different y-axis scales.

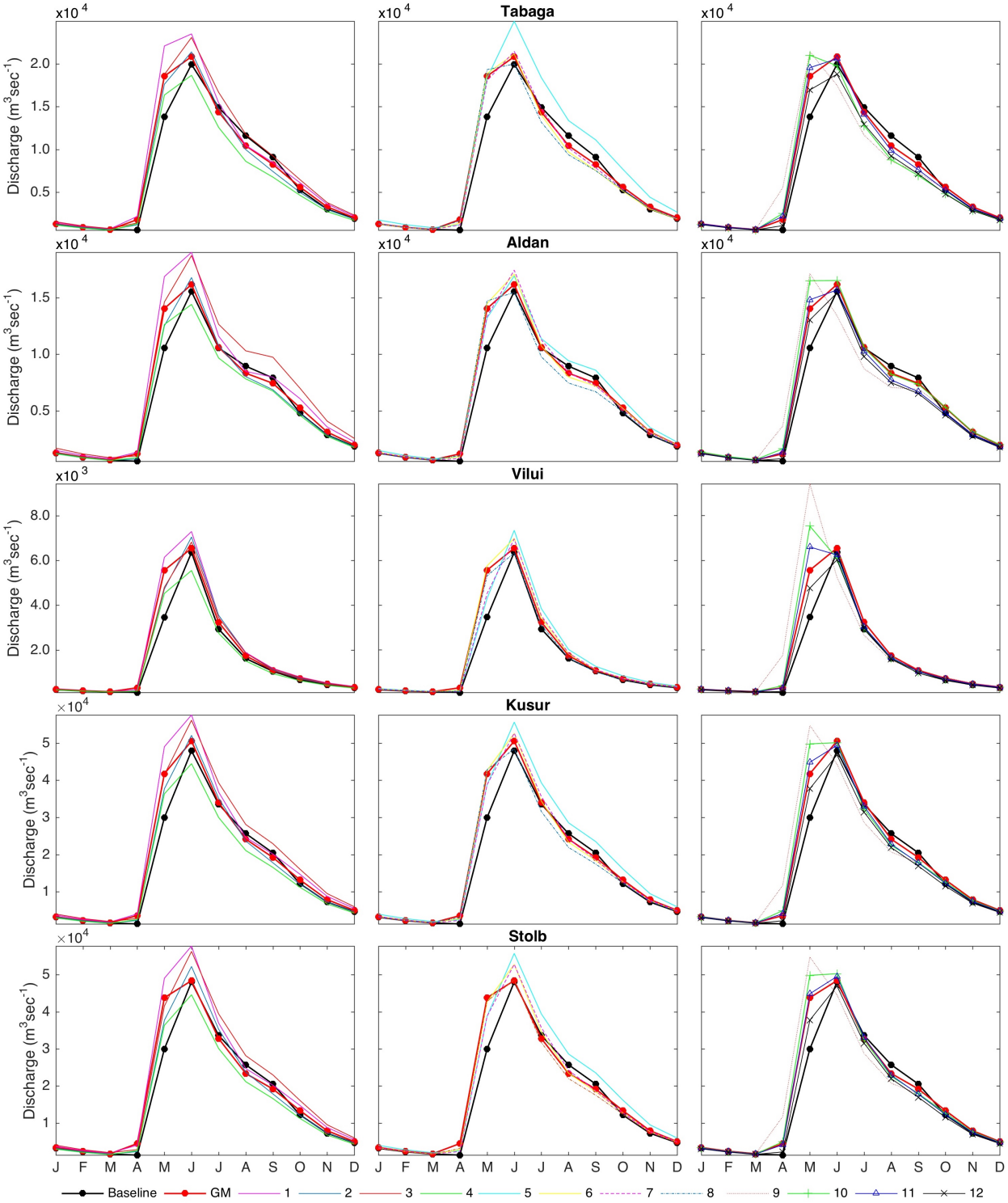

Figure 5. Mean monthly discharges at each gauging station for each scenario. The baseline (B) and group ensemble mean (GM) are shown in each figure to facilitate comparison. Note different y-axis scales for different stations.

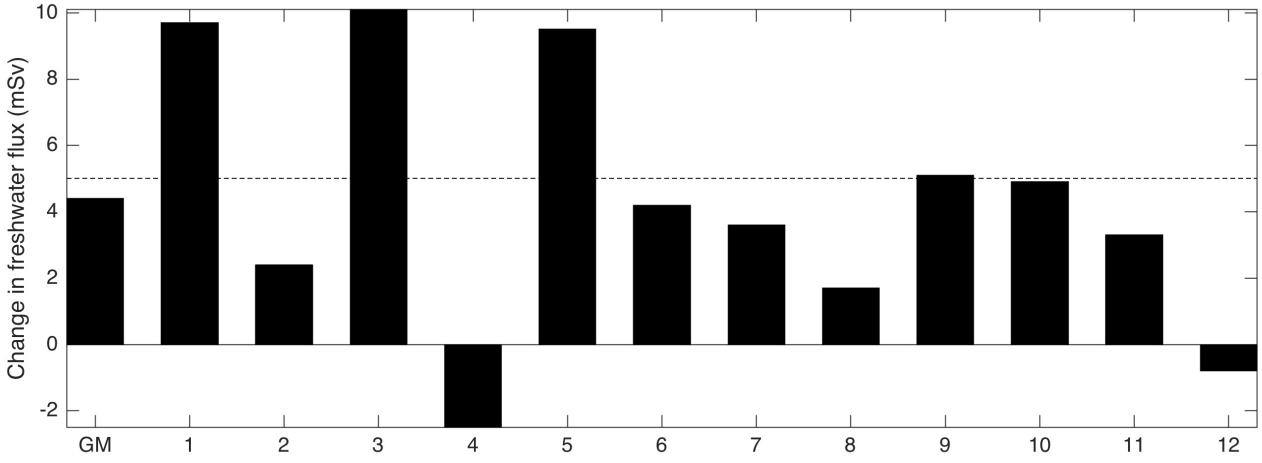

Figure 6. Projected additional annual fluxes of freshwater from the three Eurasian Rivers (Lena, Yenisei and Ob) to the Arctic Ocean for each GCM group and the group ensemble mean (GM). The dashed line represents the minimum amount required to weaken AMOC (Schulz et al. 2007; Yang et al. 2016).

649 **Author attributions**

650

651 **Charlotte E. Hudson (CEH)**, UCL Department of Geography, University College London, Gower Street,
652 London, WC1E 6BT (charlotte.hudson.15@ucl.ac.uk)

653 CEH developed the hydrological model of the Lena and undertook its calibration / validation. She
654 developed the climate change scenarios and undertook their simulation using the MIKE SHE / MIKE 11
655 model. CEH prepared the first draft of this paper.

656 **Julian R. Thompson (JRT)**, UCL Department of Geography, University College London, Gower Street,
657 London, WC1E 6BT (j.r.thompson@ucl.ac.uk)

658 JRT supervised model development, scenario creation and simulation. He provided extensive edits of
659 drafts of the manuscript.